Available online at www.sciencedirect.com
SCIENCE DIRECT
Thermochimica Acta 432 (2005) 222–228
thermochimica acta
www.elsevier.com/locate/tca

Specific heat and dielectric relaxations in ultra-thin polystyrene layers

Veronica Lupaşcu [a], Heiko Huth [b], Christoph Schick [b], Michael Wübbenhorst [a,*]

[a] *Delft University of Technology, Department of Chemical Technology, Julianalaan 136, 2628 BL Delft, The Netherlands*
[b] *Institute of Physics, University of Rostock, Universitaetsplatz 3, 18051 Rostock, Germany*

Received 10 March 2005; received in revised form 1 April 2005; accepted 5 April 2005
Available online 11 May 2005

Abstract

The effect of thickness on the glass transition dynamics in ultra-thin polystyrene (PS) films (4 nm < L < 60 nm) was studied by thin film ac-calorimetry, dielectric spectroscopy (DRS) and capacitive dilatometry (CD). In all PS-films, a prominent α-process was found in both the ac-calorimetric and dielectric response, indicating the existence of cooperative bulk dynamics even in films as thin as 4 nm. Glass transition temperatures (T_g) were obtained from ac-calorimetric data at 40 Hz and from capacitive dilatometry, and reveal a surprising, marginal thickness dependence $T_g(L)$. These results, which confirm recent data by Efremov et al. [Phys. Rev. Lett. 91 (2003)] but oppose many previous observations, is rationalized by differences in film annealing conditions together with the fact that our techniques probe exclusively cooperative dynamics (ac-calorimetry) or allow the effective separation of surface and "bulk"-type mobility (CD). Two other observations, a significant reduction in c_p towards lower film thickness and the decrease in the contrast of the dilatometric glass transition, support the idea of a layer-like mobility profile consisting of both cooperative "bulk" dynamics and non-cooperative surface mobility.

Keywords: Glass transition; Ultra-thin films; Confinement; Polystyrene; Dielectric relaxations; Thin film calorimetry

1. Introduction

Glass formation is a general property of many liquids, which are able to circumvent crystallization during cooling below their melting point (T_m) even under moderate cooling rates. In the supercooled state the relaxation times $\tau(T)$ and the viscosity $\eta(T)$ increase dramatically with decreasing temperature, a behavior that can usually be described well with the Vogel–Fulcher–Tammann (VFT) law ($\tau = \tau_0 \exp\{E_V/k(T - T_V)\}$) within the temperature range $T_g < T < T_m$. A widely accepted idea to rationalize this VFT-behavior was put forward by Adam and Gibbs (AG) based on the assumption of cooperatively rearranging regions (CRR) [1,2]. Since the AG approach does not make quantitative predictions about the characteristic length of cooperativity ξ, attempts have been undertaken to probe ξ indirectly by imposing a variable geometric confinement (characteristic dimension L) to the glass forming molecular ensemble at which the cooperative dynamics deviates from the bulk-behavior.

This idea, the study of finite size effects on the dynamic glass transition, has stimulated extensive research on various glass forming systems in nm-scale geometric confinement in the past decade. Typical confined glass forming systems comprise H-bonding liquids (ethylene glycol, propylene glycol) confined in nanoporous glasses [3], porous membranes [4], or channel structures of zeolite host systems [5,6]. For polymeric glass formers, on the other hand, finite size effects have been reported for ultra-thin polymer films [7,8], clay-based nano-composites [9] or systems that form nanophase separated alkyl domains giving rise to a "hindered" glass transition [10,11].

Since polymers enable the formation of stable freely standing or supported films and the dimension of the confining geometry is given by the film thickness, ultra-thin polymer films have become a particularly attractive model system to study finite size effects on glass transition. Another advantage of using supported thin films is that the interfacial interaction of the polymer with the substrate is readily defined. For freely

* Corresponding author. Tel.: +31 152 786940; fax: +31 152 787415.
E-mail address: wubbenhorst@tnw.tudelft.nl (M. Wübbenhorst).

0040-6031/$ – see front matter © 2005 Elsevier B.V. All rights reserved.
doi:10.1016/j.tca.2005.04.022

standing polystyrene (PS) films, spectacular glass transition temperature (T_g) reductions of more than 70 K were found, depending on the film thickness and, above a critical molecular weight, on the end-to-end distance R_{EE} of the polymer as well [12]. For supported films, much lower, but still considerable T_g reductions were observed [7,13–15].

One has to emphasize that most of the glass transition effects reported for thin polymer films were obtained by density related methods: ellipsometry [7], X-ray reflectivity [16], Brillouin light scattering [8], positron annihilation lifetime spectroscopy (PALS) [17]. More recently, other experimental techniques like dielectric spectroscopy, inelastic neutron scattering and dynamic light scattering, which reveal the polymer dynamics by sensing molecular fluctuations, are increasingly used. On first glance, these methods seem to confirm readily T_g-reductions as found by expansivity techniques [18]. Unfortunately, calorimetry methods, which are generally regarded as a decisive way to measure glass transitions in bulk materials [19], did not play so far a significant role in studies of ultra-thin polymer films until they had been reintroduced recently by Efremov and Allen [20]. The authors, who studied various polymer films spin-coated on a thin-film calorimeter, revealed basically no T_g-effects upon thickness reduction down to ∼3 nm, a finding being completely controversial to a large body of previous experimental results [20,21].

The present paper represents the first attempt to combine ac-calorimetric and dielectric methods for studying thin PS-films within a thickness range of 4 to 60 nm. Both techniques are frequency-domain methods and are characterized by wide and highly overlapping dynamic ranges that qualify them for the study of glass transition dynamics.

2. Experimental

2.1. Thin film preparation

Atactic polystyrene (Pressure Chemical Company) with an intermediate molecular mass (M_w = 160.000 g/mol) and low polydispersity (<1.06) was used in this study. Ultra-thin PS-films were prepared at Delft University by spin coating on either aluminum deposited glass slides (DRS samples) or on the SiO_2 passivated surface of the sensors used for ac-calorimetry. The film thickness was varied by changing the polymer concentration in solution (toluene) in the range from 0.15 to 1.64 weight percent. To achieve reproducible results, the same rotation speed (3000 rpm) and spinning time (20 s) were used for all samples.

After this procedure, the sensors covered with the PS layers were shipped to Germany for ac-calorimetric measurements. The samples intended for dielectric investigations were treated as follows. After annealing for 12 h at 120 °C, a second aluminum electrode was deposited using the same UHV thermal evaporation setup. This "flash" deposition was performed with the maximum possible evaporation rate (>10 nm/s) in order to minimize the diffusion of metal particles into the polymer film [22].

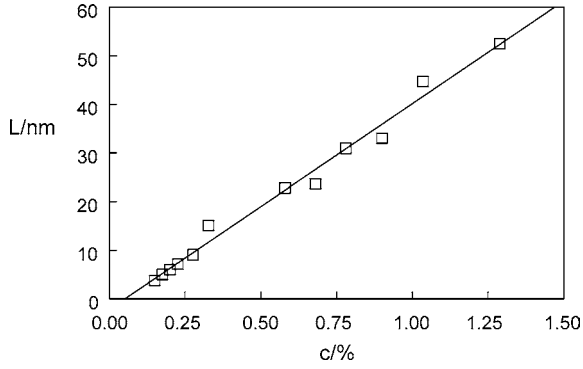

Fig. 1. Predicted (solid line) and measured (symbols) film thickness of polystyrene films as function of the concentration of the polymer solution. The experimental data were determined from capacity measurements at room temperature.

The film thicknesses were evaluated from the electrical sample capacity C', measured at room temperature, which yields the film thickness L in a straightforward way using the relation $C' = \varepsilon' \varepsilon_0 S/L$, were ε' is the permittivity of the bulk PS ($\varepsilon' = 2.5$), ε_0 is the permittivity of the vacuum, S is the area of the electrode ($S = 4\,mm^2$). The accuracy of this procedure has been verified in a previous study by using ellipsometry [23,24] and compares well with the predicted thickness values based on the concentrations of the polymer solutions (cf. Fig. 1).

2.2. Dielectric spectroscopy

Dielectric measurements in the frequency range from 10^{-1} to 10^7 Hz were performed using a high-resolution dielectric analyzer (ALPHA Analyzer, Novocontrol Technologies). The samples were first heated until 150 °C, annealed for 1 h and subsequently measured upon cooling to −20 °C at an effective rate of 0.5 K/min. All measurements took place in a nitrogen-flushed cryostat that prevents moisture uptake or oxidation during the experiments.

2.3. Thin film ac-calorimetry

A commercially available sensor, thermal conductivity gauge TCG-3880 (Xensor Integrations, NL), was utilized as a measuring cell for ac-calorimetric measurements. In the centre of a free standing 500 nm thin silicon-nitride membrane a small heater is placed. The heater consists of two parallel stripes of 50 μm distance. The temperature distribution in the area between the stripes is almost uniform as shown in [25]. Around the heater the six hot junctions of a thermopile are arranged. The heater, thermopile and conducting stripes are covered by a 700 nm silicon oxide layer for protection. The sample is spread over the whole sensor using the above-described spin coating procedure. As common in ac-calorimetry a small sinusoidal voltage is applied to the heater

to generate a periodic power in the order of μW. The resulting temperature oscillation with amplitude in the order of 0.1 K is measured by the thermopile. Only the small heated area, which can be considered as a point heat source, is of interest. For enhanced sensitivity a differential setup is used. Two sensors are placed adjacent in a thermostat at temperature T_B. Measurements are either done at a single frequency changing the temperature continuously (temperature scans) or at different frequencies keeping the temperature constant (frequency scans). In the latter case temperature can be changed stepwise. To get an almost uniform temperature distribution and small errors in temperature a heating/cooling rate of 2 K/min was used. To get the actual sample temperature the measured resistance of the membrane heater was used to monitor the temperature. All measurements were done in nitrogen at ambient pressure.

An ac-calorimeter based on a single sensor is described in detail in Ref. [26] and the differential setup used in this work in [27].

Complex heat capacity of the sample, C_S, can be obtained from the measured complex temperature amplitudes $T = \Delta U/S$ and $T_0 = \Delta U_0/S$ for the differential system with and without sample, respectively.

$$C_S = \frac{i\omega \cosh(\alpha_0)\tilde{C}_0^2}{SP}[\Delta U - \Delta U_0] \quad (1)$$

with ΔU and ΔU_0 measured complex thermopile voltage amplitude, S thermopile sensitivity, $\tilde{C}_0$ effective heat capacity of the empty cell depending on frequency and surrounding gas and a factor $\cosh(\alpha_0)$ correcting the temperature because of the distance between heater and thermopile [28]. As seen from Eq. (1), the measured differential signal amplitude ΔU of the thermopile is proportional to the heat capacity of the sample C_S. The asymmetry of the empty sensors causes an additional offset ΔU_0 to the measured signal amplitude only, which can be neglected for T_g and Δc_p measurements. Details of the setup are shown in Fig. 2.

3. Results and discussion

Due to the weak dielectric activity of PS, dielectric measurements on PS-films allow the evaluation of both the "spectroscopic" [$T_g(\alpha)$] and the volumetric glass transition temperature [T_g(dil)] from capacitive dilatometry, in one experiment.

Fig. 3 is representative for a bulk sample of PS showing the temperature dependence of the dielectric permittivity $\varepsilon'(T)$ for various frequencies between 8 and 375 kHz. It can be seen that at lower temperatures all $\varepsilon'(T)$ curves for different frequencies fall along a single line, and decrease with increasing temperature. From the kink in this unique $\varepsilon'(T)$ dependence, which is an expression of a different volume expansivity in the glass state and the amorphous melt, the dilatometric glass transition temperature T_g(dil) can be obtained [14].

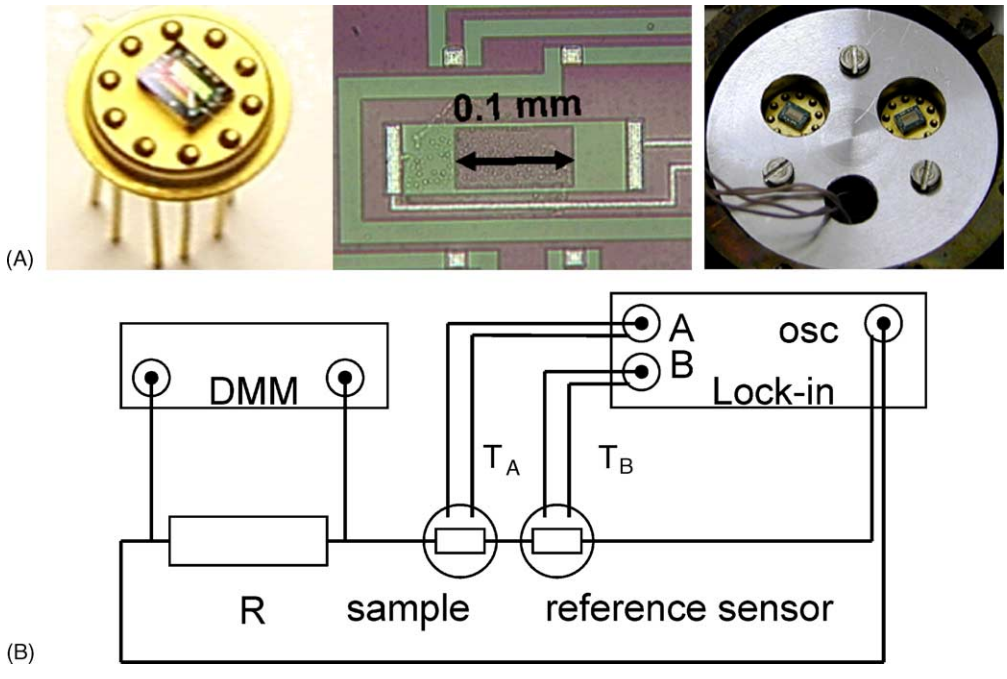

Fig. 2. (A) Scheme of the thin-film ac-calorimeter. The left hand picture shows the thermal conductive vacuum gauge from Xensor integrations NL. The middle picture shows the magnified center area of the membrane with the heater indicated by the arrow and four hot junctions of the thermopile (bright squares). The right hand picture shows the chip sensors mounted in the differential setup. The diameter of the aluminum block is 36 mm and mounted in the cryostat. (B) Scheme of the electric setup. The internal generator of the lock-in amplifier drives the heater current. The differential signal A–B of the thermopiles is analysed by the lock-in amplifier and further processed. The voltage over the known resistor R is measured with a digital multimeter to calculate the actual heater power. All components are controlled by a PC-based data acquisition system.

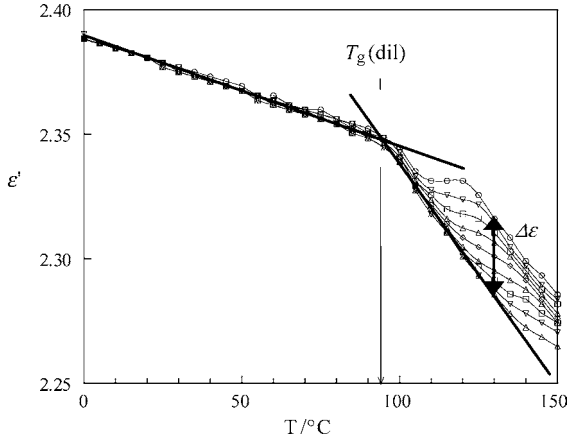

Fig. 3. The temperature dependence of the permittivity $\varepsilon'(T)$ for a bulk sample of polystyrene. The kink in $\varepsilon'(T)$ marks the dilatometric glass transition [T_g(dil)]. The frequency dependent step in $\varepsilon'(T)$ at $T > T_g$ is due to dielectric α-relaxation ($\Delta\varepsilon$: relaxation strength). The solid lines represent linear fits of the data.

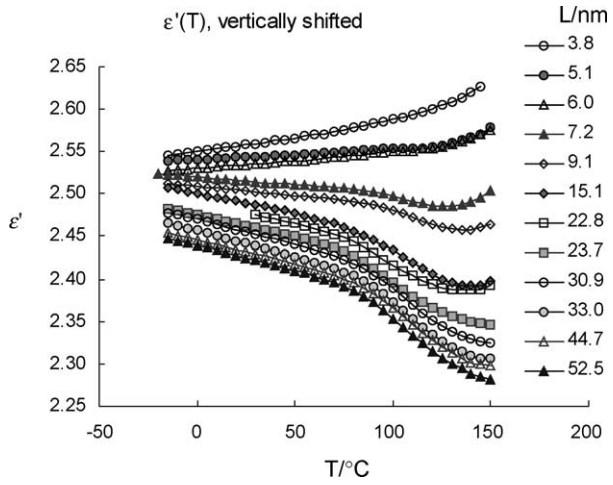

Fig. 4. Dielectric permittivity $\varepsilon'(T, f = 10\,\text{kHz})$ as function of temperature for various film thicknesses.

It should be emphasized that there is not a standard procedure to define T_g(dil) based on dilatometric curves as measured by, e.g. ellipsometry, X-ray reflectivity or capacitive dilatometry. In case of bulk samples that show narrow glass transition regions, T_g(dil) can readily be evaluated from the intersection of the linearly extrapolated data from the glass and the melt region (cf. solid lines in Fig. 3). For ultra-thin polymer films, tremendously broadened transition regions are often found, which makes the unambiguous determination of a glass transition temperature difficult.

To see the influence of the fit procedure on the T_g values, we have applied two different evaluation methods, the first of which was already described. As an alternative approach, we have used a fit equation similar to an expression proposed by Dalnoki-Veress [29], which allows the modelling of the whole $\varepsilon'(T)$ curve with a set of independent parameters for the width of the transition region (W), the characteristic transition temperature (T_g), and two quantities (M and G) that account for the temperature coefficient in the melt and in the glassy state. This procedure was proven to yield stable fit results, provided that the data show a symmetric profile around T_g.

$$\varepsilon'(T) = \varepsilon'(T_g) + (T - T_g)\left[\tanh\left(\frac{T - T_g}{w}\right)\left(\frac{M - G}{2}\right) + \left(\frac{M + G}{2}\right)\right] \quad (2)$$

The results from the both approaches are displayed in Fig. 6 later in this paper. Although there are systematic differences between the two $T_g(L)$ series by about 5 K, both series reveal the same trend and a comparable uncertainty.

The temperature dependence of the dielectric permittivity for film thicknesses in the range from 3.8 to 52.5 nm is presented in Fig. 4. At lower film thicknesses a clear broadening of the transition can be observed, though there is not a clear change in the T_g values. Another interesting feature is the change in the ("glassy") slope from negative to positive values for films thinner than 6 nm.

The ac-calorimetric data shown in Fig. 5 are obtained at a scanning rate of 2 K/min and a frequency of 40 Hz. To avoid influences of preparation and to erase sample history the second heating and cooling step are used for determining the glass transition temperature T_g. Because of missing empty measurements the thermopile signal ΔU, proportional to heat capacity, is used for data evaluation. The signal is shifted by an additional offset caused by the asymmetry of the chip sensors in the differential setup. For determination of the glass transition temperature this can be neglected. Here the temperature at half step height of ΔU can be used, which corresponds to the maximum in the phase angle or imaginary part of complex heat capacity. The glass transition temperature from ac-calorimetry shown in Fig. 5 is obtained using a tangent construction from the liquid and glassy region determining the temperature at half step of the thermopile signal as common in scanning calorimetry.

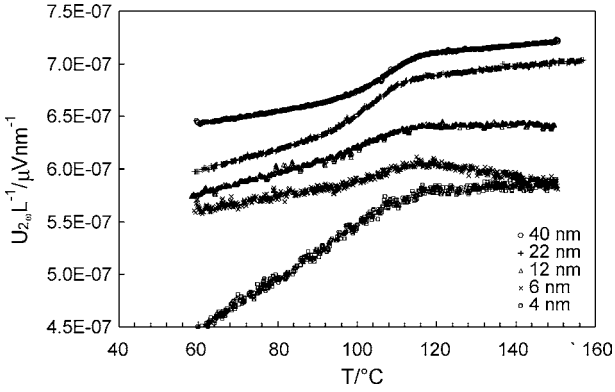

Fig. 5. Normalized ac-calorimetric response $U_2\omega/L$ as function of temperature for five different film thicknesses. The scanning rate for all measurements was 2 K/min at a frequency of 40 Hz. The data after a heating/cooling cycle 50 °C −150 °C, −50 °C with 2 K/min are used.

The step in ΔU is also not affected by the offset and is proportional to the step in heat capacity. The curves in Fig. 5 are normalized dividing the thermopile signal ΔU by the film thickness L of the polystyrene film. For the thin films under investigation probed sample mass at a given frequency depends on film thickness only. Consequently, the step at glass transition in the normalized signal is proportional to the step in specific heat capacity. For 6 nm and especially for 4 nm a change in the shape of the curves from a step to a bend-like behavior is obtained. This is a sign for a change in the dynamics of the sample and provides evidence that we measure a thin film rather than droplets due to dewetting. That no dewetting occurs on the calorimetric sensors was proven by AFM too.

The glass transition temperatures for all film thicknesses in the range from 4 to 60 nm obtained by ac-calorimetry (open triangles) and capacitive dilatometry are summarized in Fig. 6. The data reveal two main features, a systematic shift between the T_g-values originating from the different techniques, and a weak, if any, thickness dependence of the glass transition temperature, particularly for the ac-calorimetric data.

To rationalize the systematic discrepancy between T_g(dil) and $T_g(c_p)$, we have to take into account the characteristic measurement frequencies of the individual experiments. In the CD experiment, the relaxation of sample volume (here: thickness via capacity) was recorded during cooling at a rate of 0.5 K/min, which corresponds to an equivalent frequency $\sim 10^{-3}$ Hz. In contrast, the ac-calorimetric T_g's were evaluated from specific heat relaxation data measured at 40 Hz, a frequency being 4–5 decades higher, which explains the apparent "T_g"-shift of ~20 K sufficiently.

While the results from Fig. 6 confirm a good consistency between the cooperative dynamics as manifested in the specific heat and volume relaxation (CD), an analogue comparison can also be made based on the *relaxation times* of the α-process obtained from dielectric and specific heat spectroscopy. Such comparison is presented in Fig. 7, showing an excellent agreement between the relaxation time data $\tau_\alpha(T)$

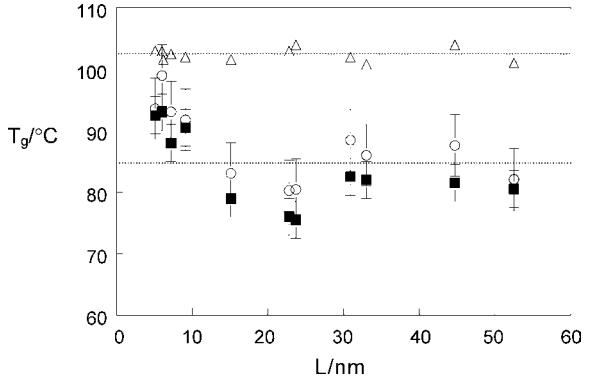

Fig. 6. Glass transition temperature as function of the film thickness. Open triangles represent results from ac-calorimetry. The filled squares and open circles correspond to data from capacitive dilatometry using two different fit procedures of $\varepsilon'(T)$ curves.

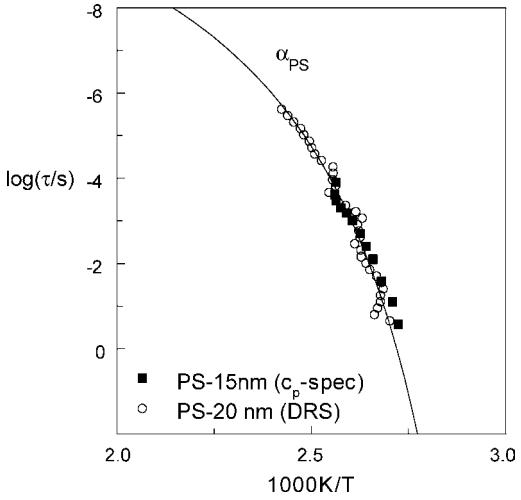

Fig. 7. Activation plot of the relaxation time τ_α determined from peak maxima in the dielectric loss $\varepsilon''(T)$ (open circles) and temperature at half step height of $\Delta U(T)$ response (filled squares).

from both techniques for samples in the order 15–20 nm in thickness. This result makes us confident that both the dielectric α-process and the specific heat relaxation data (cf. Fig. 6) probe the same cooperative fluctuations associated to the dynamic glass transition. Unfortunately, dielectric relaxation data could not be obtained for the thinnest films (<15 nm) due to increasing broadening and intensity loss of the dielectric α-process towards lower thicknesses.

We will now discuss the effect of film thickness on the glass transition temperature as shown in Fig. 6 in more detail. As mentioned before, neither the volumetric nor the ac-calorimetric data reveal a strong increase or decrease in T_g, a result that is in contradiction to observations by other authors like Fukao [14] and Kawana [15], who reported large T_g reductions with decreasing film thickness for supported PS-films. On the other hand, our findings are in line with very recent results by Efremov et al. [21] who revealed virtually no thickness dependence in the *calorimetric glass transition temperature* from fast scan measurements at about 1700 K/min for polystyrene, poly(2-vinyl pyridine) and poly(methyl methacrylate) films on a platinum surface.

Comparing our results with those from Efremov reveals interesting details:

(a) The absolute "T_g"-values from both different calorimetric methods differ by about 10 K (ac-calorimetry: ~103 °C, Efremov; fast scan 115 °C), which is due to differences in the effective measurement frequency (cf. discussion above).
(b) Closer inspection of the data from Efremov [20] shows a slight, but significant trend in the $T_g(L)$ dependence for PS (*s*-shaped curve) that was originally not discussed by the authors, which resembles strongly the *s*-shaped trend in the dilatometric T_g-values (cf. Fig. 6). In contrast, no such trend is visible in our ac-calorimetric results within the error limits.

Apart from some fine structure in the $T_g(L)$ dependences that might be the result of a complex interplay of various mechanisms like conformational changes, surface-induced chain alignment of specific polymer–substrate interactions, we should emphasize that these effects are negligible compared to the substantial T_g-reduction in the order of 30 K according to the literature [15].

Though the substrates and the methods of measurement are different for our samples and also if compared with Efremov data, we have similar results. These results do also agree with much earlier findings from Wallace [16] who reported no thickness effects on T_g for PS-films on hydrogen terminated silicon substrates studied by X-ray reflectivity. However, there is a clear disagreement with some previous results reported by some of the authors of this paper [30] and data from Fukao [13], Forrest and Kawana [15], who reported large T_g reductions for supported PS film that apparently support the idea of a layer-like mobility profile assumed by various authors.

We think that the contradictive observation of a *thickness independent* glass transition temperature has a rational basis and involves two main issues, *mixing* of surface and "bulk"-dynamics in the experimental response, and *improper annealing* of the sample films. The first problem reflects the general dilemma of any dilatometric technique, e.g. ellipsometry that the experimental response $L(T)$ represents the entire sample thickness (or volume), without discriminating between effects that might originate from different sample regions (surface, core etc.).

In case of a common layer scenario that assumes a "bulk"-type central layer in series with a "liquid"-like surface layer, it is likely that there exist two individual freezing temperatures ($T_{f,\,surf}$: surface, $T_{g,\,bulk}$: central layer) that both contribute to the overall experimental response $L(T)$ (cf. Fig. 8). It is clear that an attempt to model the $L(T)$ data by a single glass transition process will necessarily lead to an apparent glass transition temperature that actually represents a "mixed" glass transition temperature. This phenomenon has been addressed in Ref. [30], which showed an apparent divergence between the T_g-values from CD and glass transition temperatures derived from the dielectric α-process. Fig. 8 illustrates further that the existence of a surface relaxation would manifest differently in the volumetric (left) and dielectric response (right). While unfreezing of a liquid upon heating always lead to a reduction in density, the two individual dielectric responses $\varepsilon'_{surf}(T)$ and $\varepsilon'_{core}(T)$ are characterized by opposite trends, provided that the surface response $\varepsilon'_{surf}(T)$ is dominated by a dielectric relaxation process. Superimposing these two contributions, weighted by the relative thickness of the core and surface layer, will result in a $\varepsilon'(T)$ dependence as confirmed by our experimental results given in Fig. 4. Here, a continuous tilt of the $\varepsilon'(T)$ curve towards lower thickness can be seen, accompanied by a reduction in the strength of the glass transition indicated by the kink. Although the model put forward in Fig. 8 does not explicitly refute a cooperative mechanism for the enhanced surface mobility, there are strong hints for a non-cooperative behavior coming from dielectric spectroscopy [30,31]. In a recent paper, we have shown that for thin films around $L \sim 8$ nm, an additional relaxation process is discernible that shows Arrhenius parameters being typical for a local relaxation [30]. Such a second process, which is likely hidden in many published ellipsometric data, was not found in calorimetric studies confirming that this process involves no c_p-relevant cooperative fluctuations. Hence, we think that the cooperative dynamics in ultrathin PS-films can be fully assigned to the core layer showing basically bulk-dynamics. Inspecting the c_p data normalized to the film thickness given in Table 1 yields significant reductions in c_p/L towards lower

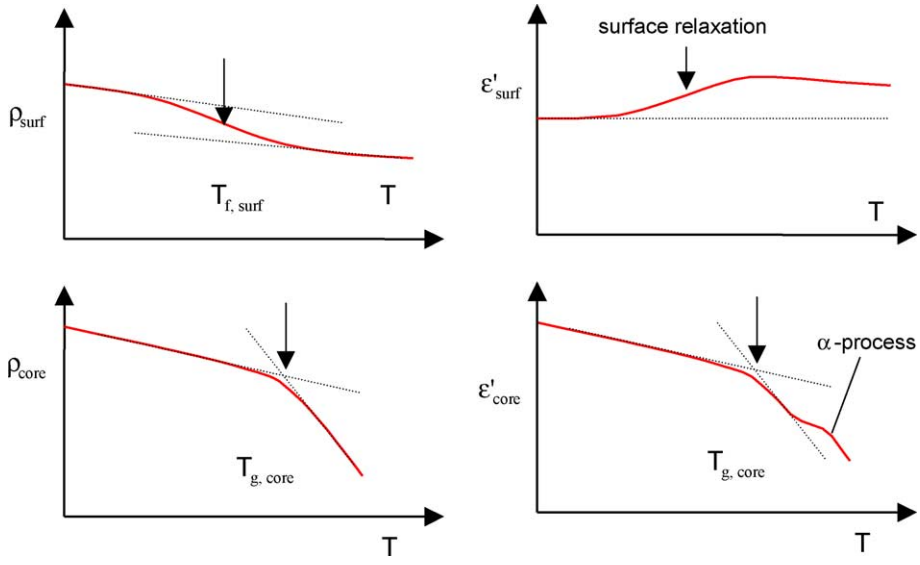

Fig. 8. Schematic representation of layer-specific temperature dependences of the density $\rho(T)$ (left) and dielectric constant $\varepsilon'(T)$. Top: response from the surface layer (freezing temperature $T_{f,surf}$), bottom: bulk-type response of the central layer ($T_{g,\,core}$).

Table 1
Normalized specific heat of PS-films

Thickness (L/nm)	c_p (L^{-1}/a.u.)
4 ± 0.5	0.020 ± 0.005
6 ± 0.6	0.020 ± 0.005
8 ± 0.8	0.036 ± 0.004
12 ± 1.0	0.041 ± 0.004
15 ± 1.5	0.031 ± 0.004
22 ± 2.0	0.039 ± 0.004
30 ± 3.0	0.043 ± 0.004
40 ± 4.0	0.033 ± 0.004

film thickness, which is also in line with a surface layer having no cooperative dynamics. However, the evolution of a clear-cut mobility profile as suggested by the data in the present work, should be sensitive to the annealing conditions that will decide over which thickness range a local equilibrium of the polymer configuration can be attained. A detailed treatment of this issue will be subject of a forthcoming paper.

4. Conclusions

The thickness effect on the glass transition dynamics in ultra-thin polystyrene films was examined by thin film ac-calorimetry, dielectric spectroscopy and capacitive dilatometry. A prominent α-process was found in all PS-films, both in the calorimetric and dielectric response. This is an indication for the existence of cooperative bulk dynamics even in films as thin as 4 nm. Glass transition temperatures (T_g) from ac-calorimetric data and from capacitive dilatometry revealed a more or less thickness *independence* in $T_g(L)$.

First, these findings confirm recent results by Efremov [32], however come in contradiction to many previous observations. This can be rationalized by differences in film annealing conditions together with the fact that our techniques probe exclusively cooperative dynamics (ac-calorimetry) or allow the effective separation of surface and "bulk"-type mobility (CD). Two other observations, a significant reduction in c_p towards lower film thickness and the decrease in the contrast of the dilatometric glass transition, support the idea of a layer-like mobility profile consisting of both cooperative "bulk" dynamics and non-cooperative surface mobility.

Acknowledgements

One of the authors (V.L.) would like to thank to FOM for financial support. H. Huth acknowledges financial support form the German Science Foundation (DFG).

References

[1] G. Adam, J.H. Gibbs, J. Chem. Phys. 43 (1965) 139.
[2] E. Donth, J. Non-Cryst. Solids 307 (2002) 364–375.
[3] P. Pissis, A. Kyritsis, G. Barut, R. Pelster, G. Nimtz, J. Non-Cryst. Solids 235 (1998) 444–449.
[4] G.P. Crawford, D.K. Yang, S. Zumer, D. Finotello, J.W. Doane, Phys. Rev. Lett. 66 (1991) 723–726.
[5] A. Huwe, F. Kremer, P. Behrens, W. Schwieger, Phys. Rev. Lett. 82 (1999) 2338–2341.
[6] M. Wübbenhorst, G.J. Klap, J.C. Jansen, H. van Bekkum, J. van Turnhout, J. Chem. Phys. 111 (1999) 5637–5640.
[7] J.L. Keddie, R.A.L. Jones, R.A. Cory, Europhys. Lett. 27 (1994) 59–64.
[8] J.A. Forrest, K. DalnokiVeress, J.R. Stevens, J.R. Dutcher, Phys. Rev. Lett. 77 (1996) 2002–2005.
[9] S.H. Anastasiadis, J. De Physique Iv 10 (2000) 255–258.
[10] M. Beiner, H. Huth, Nature Mater. 2 (2003) 595–599.
[11] Z. Yildirim, M. Wübbenhorst, E. Mendes, S.J. Picken, I. Paraschiv, A.T.M. Marcelis, H. Zuilhof, E.J.R. Sudhölter, J. Non-Cryst. Solids, 2005, in press.
[12] J. Mattsson, J.A. Forrest, L. Borjesson, Phys. Rev. E 62 (2000) 5187–5200.
[13] K. Fukao, S.B. Uno, Y. Miyamoto, A. Hoshino, H. Miyaji, J. Non-Cryst. Solids 307 (2002) 517–523.
[14] K. Fukao, Y. Miyamoto, Phys. Rev. E 61 (2000) 1743–1754.
[15] S. Kawana, R.A.L. Jones, Phys. Rev. E 63 (2001) no. 021501.
[16] W.E. Wallace, J.H. van Zanten, W.L. Wu, Phys. Rev. E. 52 (1995) 3329–3332.
[17] G.B. DeMaggio, L. Xie, W.E. Frieze, D.W. Gidley, M. Zhu, H.A. Hristov, A.F. Yee, Phys. Rev. Lett. 78 (1997) 1524–1527.
[18] K. Fukao, Y. Miyamoto, J. De Physique Iv 10 (2000) 243–246.
[19] J.E. Mark, AIP Press, Woodbury, NY, 1996.
[20] M.Y. Efremov, E.A. Olson, M. Zhang, Z. Zhang, L.H. Allen, Phys. Rev. Lett. 91 (2003).
[21] M.Y. Efremov, E.A. Olson, M. Zhang, Z.S. Zhang, L.H. Allen, Macromolecules 37 (2004) 4607–4616.
[22] V. Zaporojtchenko, T. Strunskus, K. Behnke, C. von Bechtolsheim, A. Thran, F. Faupel, Microelectron. Eng. 50 (2000) 465–471.
[23] M. Wübbenhorst, C.A. Murray, J.A. Forrest, J.R. Dutcher, 11th International Symposium on Electrets 1–3 October (Ed.: R. Fleming), IEEE Service Center Piscataway Melbourne N.J. Australia, 2002, pp. 401–406.
[24] M. Wübbenhorst, V. Lupascu, Phys. Rev. E, 2005, submitted for publication.
[25] A.A. Minakov, S.A. Adamovsky, C. Schick, TCA, this issue.
[26] A.A. Minakov, S.B. Roy, Y.V. Bugoslavsky, L.F. Cohen, Rev. Sci. Instr. 76 (2005) 043906.
[27] H. Huth, A.A. Minakov, C. Schick, Netsu Sokutei 32 (2005) 69.
[28] A.A. Minakov, Y.V. Bugoslavsky, C. Schick, Thermochim. Acta 317 (1998) 117.
[29] C.B. Roth, B.G. Nickel, J.R. Dutcher, K. Dalnoki-Veress, Rev. Scientific Instr. 74 (2003) 2796–2804.
[30] V.R. Lupascu, M. Wübbenhorst, JNCS, submitted for publication.
[31] K. Fukao, Y. Miyamoto, Phys. Rev. E 6401 (2001) 1803.
[32] M.Y. Efremov, E.A. Olson, M. Zhang, L.H. Allen, Thermochim. Acta 403 (2003) 37–41.